J. Fluid Mech. (1997), *vol.* 337, *pp.* 103–128

A composite asymptotic model for the wave motion in a steady three-dimensional subsonic boundary layer

By OLEG S. RYZHOV[1] AND EUGENE D. TERENT'EV[2]

[1]Department of Mathematical Sciences, Rensselaer Polytechnic Institute, Troy, NY 12180-3590, USA

[2]Computing Center, Russian Academy of Sciences, 40 Vavilov Street, 117333 Moscow, Russian Federation

(Received 4 November 1995 and in revised form 29 October 1996)

The problem for a thin near-wall region is reduced, within the triple-deck approach, to unsteady three-dimensional nonlinear boundary-layer equations subject to an interaction law. A linear version of the boundary-value problem describes eigenmodes of different nature (including crossflow vortices) coupled together. The frequency ω of the eigenmodes is connected with the components k and m of the wavenumber vector through a dispersion relation. This relation exhibits two singular properties. One of them is of basic importance since it makes the imaginary part $\mathrm{Im}(\omega)$ of the frequency increase without bound as k and m tend to infinity along some curves in the real (k, m)-plane. The singularity turns out to be strong, rendering the Cauchy problem ill posed for linear equations.

Accounting for the second-order approximation in asymptotic expansions for the upper and main decks brings about significant alterations in the interaction law. A new mathematical model leans upon a set of composite equations without rescaling the original independent variables and desired functions. As a result, the right-hand side of a modified dispersion relation involves an additional term multiplied by a small parameter $\varepsilon = R^{-1/8}$, R being the reference Reynolds number. The aforementioned strong singularity is missing from solutions of the modified dispersion relation. Thus, the range of validity of a linear approximation becomes far more extended in ω, k and m, but the incorporation of the higher-order term into the interaction law means in essence that the Reynolds number is retained in the formulation of a key problem for the lower deck.

1. Introduction

In recent years the rising cost of fuel has focused research attention on the total drag force, since substantial savings are possible if the boundary layer can be maintained in the laminar state at cruise. Therefore, there is currently strong interest in the problem of boundary-layer instability and transition on swept wings of aircrafts operating at high Reynolds numbers. However stability properties of a steady three-dimensional boundary-layer flow are quite different from those of the corresponding two-dimensional flow where they manifest themselves in the form of travelling self-excited Tollmien–Schlichting (TS) waves. Typical three-dimensional flows of practical importance including swept wings, cones at incidence, and rotating disks exhibit a rich variety of routes to instabilities that are generic to more complicated motions of a viscous fluid. For instance, the flow over a swept wing is susceptable to four types of instabilities, eventually leading to transition. They are leading-edge instability and contamination, centrifugal instability stemming from the blunt-nose curvature, streamwise TS instability and crossflow instability. The first two are more specific: centrifugal instability does not come into play at all if the wing is a flat swept wedge. The latter two types are general and, perhaps, a consistent characteristic of the instabilities suffered by three-dimensional boundary layers is the presense of streamwise vortices in the velocity field.

Insofar as crossflow instability is peculiar to three-dimensional shear flows and is absent from the corresponding two-dimensional flows it merits some further comments. The discovery of the crossflow instability is often attributed to Gray (1952) who found closely spaced stationary streaks in the direction of a local external stream in flight tests with a yawed wing. Shortly after his observations Gregory, Stuart & Walker (1955) put the work on stability properties of three-dimensional boundary layers on the firm basis of a linear small-disturbance theory. The key element of the theory is a transformation by Squire (1933) reducing the three-dimensional temporal stability problem to a two-dimensional one. Since that time a lot of calculations have been performed for the boundary-layer flows over swept wings and rotating disks. For the most part computer programs are designed to start with solving the initial value problem which gives the temporal development of disturbances in the unstable boundary layer on the assumption that it can be treated as quasi-parallel. However, an important feature of three-dimensional viscous shear flows is that streamwise TS instability and crossflow instability can be coupled together thus making the mathematical analysis and experimental identification of each of them an extremely challenging problem. According to Poll (1985) and Nitschke-Kowsky & Bippes (1988) coexisting travelling waves originate at approximately the same chordwise station as where the crossflow instability first appears. Recent results of Lingwood (1995) published when the present paper was in the process of being reviewed point to absolute instability of the rotating-disk flow.

The final step of the transition-prediction method based on the linear stability approach calls for an e^N-factor where the value of N is to be inferred from both wind-tunnel and flight tests. The e^N-transition-prediction scheme has been independently invented by Smith & Gamberoni (1956) and Van Ingen (1956) as applied to two-dimensional flows. However, the principal routes to transition in a two-dimensional boundary layer are milder, usually exhibiting a long distance of the linear amplification. In three-dimensional boundary layers nonlinearity comes into play at very early stages of the disturbance development. According to Hefner & Bushnell (1980) the exponent N varies depending on environmental disturbances: roughly speaking its value can be estimated as being of order 10. Details of the parallel-stability problem formulation, physical mechanisms controlling instabilities of different types, mathematical techniques involved, and results obtained are available in Mack (1984), Arnal (1986), Arnal & Juillen (1987) and Reed & Saric (1989).

An asymptotic approach to posing hydrodynamic stability problems leans upon the concept of an interactive boundary layer where the pressure variations and the displacement thickness are to be evaluated simultaneously. As applied to three-dimensional viscous shear flows, this approach has been put forward by Cebeci & Stewartson (1980). Asymptotic simplifications arising within the triple-deck theory are discussed by Manuilovich (1983), whereas Stewart & Smith (1987) shed more light on some effects of the travelling TS waves and crossflow disturbances, with particular emphasis placed on the steady eigenmodes. An analysis along these lines is set forth in Ryzhov & Terent'ev (1991) where the eigenmodes of different nature are coupled through a unified dispersion relation. A plane formed by two real wavenumbers in the local streamwise and spanwise directions serves to establish singular features, one of which being of fundamental significance. To be specific, the imaginary part of the frequency grows without bound as values of the wavenumbers tend to infinity along some curves in this plane. The singularity turns out to be strong enough to make the Cauchy problem ill posed in the linear approximation. For convenience the causes of the singularity in question are reconsidered below as the starting point for the development of an appropriate asymptotic model where the imaginary part of the eigenmode frequencies remains bounded in the whole plane of the real wavenumbers.

The geometry of a solid body in the asymptotic model is chosen as simple as possible. The idea is to take advantage of a swept flat plate where the crossflow in the near-wall region originates owing to a pressure gradient imposed from outside. Experimentally, the infinite swept condition with no variations of the stationary pressure distribution or the external velocity field in the spanwise direction is achieved by inserting appropriately contoured end-plates (Saric & Yeates 1985; Nitschke-Kowsky & Bippes 1988; Kachanov, Tararykin & Fedorov 1990). This technique appears to be especially helpful in discriminating between the centrifugal (Görtler) instability stemming from the blunt-nose curvature of a wing and the crossflow instability with vortices all rotating in the same direction. In what follows the solid body surface is assumed to be a swept flat plate with a given external pressure gradient that builds up the three-dimensional velocity field within the boundary layer.

A composite asymptotic model is advanced to provide a unified treatment of regular oscillations with moderate values of the frequency and wavenumbers as well as the aforementioned extreme when both wavenumbers tend to infinity giving rise to an unbounded increase of the amplitude growth rate. Alterations introduced in the interaction law relating the self-induced pressure to the instanteneous displacement thickness are the cornerstone of the new approach that involves a small parameter $\varepsilon = R^{-1/8}$ of the conventional triple-deck theory. Centrifugal forces supported by highly curved streamsurfaces in the main deck play an important part in the modified interaction law. However, the triple-deck structure of the disturbance field remains intact as a whole and lays the groundwork for the extended asymptotic theory. A dispersion relation is analysed to reinforce the statement that the triple-deck singularity entering the linear approximation is missing from it if $\varepsilon \neq 0$. A relevant correction term included in the interaction law comes automatically into operation to alleviate and smear out the singular behaviour of eigenmodes in the limiting case. Computed results exhibit a very strong dependence on ε even in the range of moderate wavenumbers. This is especially true with regard to the limiting case of crossflow instability leading to the jet-like near-wall fluid motion in the spanwise direction.

The local Reynolds number R is based on a reference length L^* associated with a specific point on the plate, the free-stream velocity U_∞^*, density ρ_∞^* and viscosity μ_∞^* just outside the boundary layer. Only subsonic flows are under consideration, so the Mach number $M_\infty < 1$. The time t' and Cartesian coordinates (x', y', z') are non-dimensionalized with respect to L^*/U_∞^* and L^*, respectively; the x'-axis is aligned with the direction of the local free stream, y' stands for the normal distance and z' defines the local spanwise direction (which is not necessarily parallel to the leading edge). The corresponding non-dimensional velocities (u', v', w') are based on U_∞^*, and their profiles $U_{xo}(y_2), 0, U_{zo}(y_2)$, where $y' = R^{-1/2}y_2$, determine the boundary-layer properties, U_{zo} being the crossflow in a sense which is most commonly in use (Reed

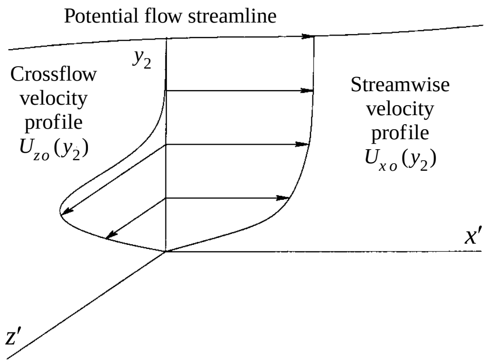

FIGURE 1. Schematic of velocity components in a three-dimensional boundary layer illustrating the definition of crossflow. The x'-axis of a Cartesian frame of reference is aligned with the direction of the local potential flow, the z'-axis points in the spanwise direction.

& Saric 1989). A schematic view of the mainflow and crossflow velocities is given in figure 1. In the frame of reference adopted both wall shear stresses $\mathrm{d}U_{xo}(0)/\mathrm{d}y_2$, $\mathrm{d}U_{zo}(0)/\mathrm{d}y_2$ are non-zero, on the other hand $U_{zo} \to 0$ as $y_2 \to \infty$. Given that a ratio μ^*/μ^*_∞ of viscosities is expressed in terms of a ratio T^*/T^*_∞ of temperatures by the Chapman linear law $\mu^*/\mu^*_\infty = C(T^*/T^*_\infty)$, the normalized wall shear stresses

$$\tau_x \tau_w = C^{1/2} \frac{T^*_w}{T^*_\infty} \frac{\mathrm{d}U_{xo}(0)}{\mathrm{d}y_2}, \quad \tau_z \tau_w = C^{1/2} \frac{T^*_w}{T^*_\infty} \frac{\mathrm{d}U_{zo}(0)}{\mathrm{d}y_2} \qquad (1.1a,b)$$

with $\tau_x^2 + \tau_z^2 = 1$, turn out to be of prime importance in the triple-deck approach (see for example Stewartson 1969; Stewart & Smith 1987; Ryzhov & Terent'ev 1991). The plate is assumed to be thermaly insulated, and so the subscript w in (1.1a,b) refers to adiabatic conditions. The density ρ' and excess pressure p' are non-dimensionalized with respect to ρ^*_∞ and $\rho^*_\infty U^{*2}_\infty$, respectively, and $R_0(y_2)$ denotes the density profile in the boundary layer with $\mathrm{d}R_0(0)/\mathrm{d}y_2 = 0$.

Conventional triple-deck arguments set forth in §2 result in boundary-layer equations. However, the leading terms of these equations are supplemented by some correction terms in order to facilitate an analysis of possible singularities. The linear approximation is introduced in §3. A discussion of a dispersion relation connecting the frequency of eigenmodes with two wavenumbers follows in §4 in the classical triple-deck framework. The limiting case of short-scaled jet-like disturbances is treated in §5 to show that centrifugal forces arising owing to highly curved streamsurfaces in the main deck are of prime importance for mitigating the corresponding triple-deck singularity. Then a new composite asymptotic model is formulated in §6; it leans upon alterations in the interaction law and involves, as a consequence, a small parameter $\varepsilon = R^{-1/8}$ in an explicit form. The triple-deck singularity turns out to be suppressed in the context of the composite model that covers moderate as well as indefinitely large values of both wavenumbers. Concluding remarks in §7 demonstrate the suitability of the Korteweg–de Vries equation for investigation of larger oscillations.

2. Equations of the wave motion

We begin with the conventional asymptotic triple-deck approach as applied to the analysis of boundary-layer stability properties in the general three-dimensional context. Thus, the disturbance pattern with pertinent scaling of both independent variables and desired functions in terms of a small parameter $\varepsilon = R^{-1/8}$, R being the local Reynolds number, is supposed to be known from the earlier work in this area (see for example Stewartson 1969; Messiter 1970; Smith, Sykes & Brighton 1977; Stewart & Smith 1987, among others). However, as Ryzhov & Terent'ev (1991) indicated, the triple-deck theory has intrinsic flaws which manifest themselves in the form of two singularities. The first singularity causes the eigenmode frequency to indefinitely grow when the oscillation wavenumbers in the local streamwise and spanwise directions attain some real finite values. The second, and much stronger, singularity results in predicting amplitude amplification rates which prove to increase without bound in the limit as values of the two wavenumbers tend to infinity according to a certain law. Aiming to obviate this evident shortcoming of the triple-deck scheme we choose to retain in asymptotically simplified equations of fluid motion the main second-order term without rescaling time, space variables, velocity-vector components and thermodynamical entities within the frequency/wavenumber range where the triple-deck theory fails to correctly predict the wave-system development.

An estimation for the time scale adopted in the triple-deck approach is $O(\varepsilon^2)$ whereas the local streamwise and spanwise length scales are both $O(\varepsilon^3)$. The latter is short compared to the $O(1)$ scale over which the base steady flow varies but large compared to the $O(\varepsilon^4)$ boundary-layer thickness. Accordingly, we introduce two sets of independent variables

$$t' = \varepsilon^2 t_m = \varepsilon^2 \tau_w^{-3/2} C^{1/4} (T_w^*/T_\infty^*) t, \tag{2.1a}$$

$$(x', z') = \varepsilon^3 (x_m, z_m) = \varepsilon^3 \tau_w^{-5/4} C^{3/8} (T_w^*/T_\infty^*)^{3/2} (x, z), \tag{2.1b}$$

where the factors τ_w, C and T_w^*/T_∞^* are used to normalize the resulting equations in the upper and lower sublayers. On the other hand, no attempt is made to incorporate the local outer-stream Mach number $M_\infty < 1$ into the affine transformation (2.1*a*, *b*) since the dependence on a difference $1 - M_\infty^2$ is generic to disturbances propagating through a three-dimensional boundary layer and therefore it cannot be ruled out from controlling equations and matching conditions even in the leading-order approximation (Stewart & Smith 1987; Ryzhov & Terent'ev 1991).

In the upper sublayer the normal coordinate y' is stretched by means of

$$y' = \varepsilon^3 \tau_w^{-5/4} C^{3/8} \left(T_w^*/T_\infty^*\right)^{3/2} y_1 \tag{2.2}$$

and the velocity field as well as density and pressure variations have the following asymptotic representation:

$$(u' - 1, v', w', \rho' - 1, p') = \varepsilon^2 \tau_w^{1/2} C^{1/4} (u_1, v_1, w_1, \rho_1, p_1) \tag{2.3}$$

which does not involve the ratio T_w^*/T_∞^* of temperatures. Upon substituting (2.1)–(2.3) into the governing Navier–Stokes equations we arrive at a system of simplified equations where the main second-order terms are expressed through the time-derivatives of the velocity components or thermodynamical entities multiplied by a new small parameter $\varepsilon_1 = \varepsilon \tau_w^{1/4} C^{1/8} \left(T_w^*/T_\infty^*\right)^{1/2}$. With ε_1 put to zero, these equations reduce to the leading-order equations considered in the conventional triple-deck approach, whereas the time-derivative terms are shifted to the second-order approximation. However, allowing for unsteadiness of the wave motion in the upper sublayer might be expected to lead in some cases to a profound destabilizing effect on the laminar state of a boundary layer.

The system of equations controlling the fluid motion in the upper sublayer can be simplified still further. A relation $\rho_1 = M_\infty^2 p_1$ valid to within second-order accuracy means that the pressure and density variations obey the adiabatic law. Then, the velocity field has a potential φ_1 such that $u_1 = \partial\varphi_1/\partial x, v_1 = \partial\varphi_1/\partial y_1, w_1 = \partial\varphi_1/\partial z$. As a result three of the asymptotically simplified equations reduce to the single Lagrange–Cauchy integral

$$p_1 = -\varepsilon_1 \frac{\partial\varphi_1}{\partial t} - \frac{\partial\varphi_1}{\partial x}. \tag{2.4}$$

With (2.4) taken into account, an equation for φ_1 is easily deducible from the remaining equations of motion in the form

$$2\varepsilon_1 M_\infty^2 \frac{\partial^2\varphi_1}{\partial t\partial x} - \left(1 - M_\infty^2\right) \frac{\partial^2\varphi_1}{\partial x^2} - \frac{\partial^2\varphi_1}{\partial y_1^2} - \frac{\partial^2\varphi_1}{\partial z^2} = 0. \tag{2.5}$$

The mixed time–space derivative $\partial^2\varphi_1/\partial t\partial x$ here proved to be of crucial significance in extending instability properties of a boundary layer in the transonic regime from high subsonic to moderate supersonic velocities (Ryzhov 1993). However, for incompressible fluid (in the limit as $M_\infty \to 0$) the unsteady term drops out of (2.5) with the consequence that φ_1 is defined by the Laplace equation. The same equation still holds within the entire subsonic regime where $(1 - M_\infty^2) = O(1)$. Thus, upon neglecting $\varepsilon_1\partial\varphi_1/\partial t$ in (2.4), we are left with a relation

$$p_1 = \frac{1}{2\pi} \int_{-\infty}^{\infty} \mathrm{d}\xi \int_{-\infty}^{\infty} \frac{\partial^2\varphi_1(t, \xi, 0, \zeta)/\partial\xi\partial y_1}{\left\{(x-\xi)^2 + \left(1 - M_\infty^2\right)\left[y_1^2 + (z-\zeta)^2\right]\right\}^{1/2}} \mathrm{d}\zeta \tag{2.6}$$

which gives p_1 in terms of the normal derivative $\partial\varphi_1/\partial y_1$ defined on the plane $y_1 = 0$.

When analysing the disturbance behaviour in the main deck, the most convenient way is to work with the unstretched independent variables t_m, x_m, z_m and the normal coordinate $y' = \varepsilon^4 y_2$ typical of the classical boundary-layer theory of Prandtl. The scalings of the desired functions,

$$\left[u' - U_{xo}(y_2), w' - U_{zo}(y_2), \rho' - R_0(y_2)\right] = \varepsilon(u_2, w_2, \rho_2), \tag{2.7a}$$

$$(v', p') = \varepsilon^2(v_2, p_2), \tag{2.7b}$$

are directly taken from the triple-deck consideration. In (2.7*a*) distributions of the velocity components U_{xo}, U_{zo} and density R_0 are assumed to be known from a solution of the global problem specifying a stationary boundary layer on a flat surface. Hence, the crossflow U_{zo} develops because of the pressure gradient imposed from outside by any artificial device. Owing to the special choice of the coordinate axes x', z' as shown in figure 1, we have $U_{xo} \to 1, U_{zo} \to 0$ as $y_2 \to \infty$ in keeping with the crossflow definition in Reed & Saric (1989) that is common to most theoretical and experimental studies.

Substitution of the asymptotic sequences (2.7*a, b*) into the original Navier–Stokes equations with allowance made for scalings (2.1*a, b*) of independent variables t_m, x_m, z_m yields a system of approximate equations comprising the leading-order and main correction terms. The contribution to the higher-order terms comes from two sources. The first one again comes from the time-derivatives of all the required functions. As in the upper sublayer, these derivatives may be disregarded provided that we restrict our consideration to the strong singularity in the amplitude growth rates and assume $\left(1 - M_\infty^2\right) = O(1)$. The second source relates to the spatial derivatives $\partial p_2/\partial x_m$ and

$\partial p_2/\partial z_m$ of the pressure along both directions in a plane parallel to the solid flat surface. But the most conspicuous feature of the system in question is that the normal pressure gradient is retained in

$$\varepsilon U_{xo}\frac{\partial v_2}{\partial x_m}+\varepsilon U_{zo}\frac{\partial v_2}{\partial z_m}=-\frac{1}{R_0}\frac{\partial p_2}{\partial y_2} \tag{2.8}$$

rather than being equated with zero. A highly stabilizing effect exerted by the normal pressure gradient on the TS eigenmodes is known from the study by Ryzhov (1993) of two transonic regimes peculiar to laminar boundary-layer flows. As distinct from the latter two-dimensional case, the normal pressure gradient in (2.8) has an additional component $U_{zo}\partial v_2/\partial z_m$ of the centrifugal force depending on the magnitude of the crossflow U_{zo}. We shall see below that this component stabilizes the crossflow vortices, suppressing their excitation at finite values of Reynolds number R (and ε).

The system of equations governing the disturbance pattern in the main deck can be reduced to two equations for the functions v_2 and p_2. Eliminating ρ_2, u_2 and w_2 between the equations of motion yields

$$\begin{aligned}U_{xo}\frac{\partial^2 v_2}{\partial x_m\partial y_2}+U_{zo}\frac{\partial^2 v_2}{\partial z_m\partial y_2}-\frac{\mathrm{d}U_{xo}}{\mathrm{d}y_2}\frac{\partial v_2}{\partial x_m}-\frac{\mathrm{d}U_{zo}}{\mathrm{d}y_2}\frac{\partial v_2}{\partial z_m}\\+\varepsilon M_\infty^2\left[\left(U_{xo}^2-\frac{1}{M_\infty^2R_0}\right)\frac{\partial^2 p_2}{\partial x_m^2}+2U_{xo}U_{zo}\frac{\partial^2 p_2}{\partial x_m\partial z_m}+\left(U_{zo}^2-\frac{1}{M_\infty^2R_0}\right)\frac{\partial^2 p_2}{\partial z_m^2}\right]=0.\end{aligned} \tag{2.9}$$

Being coupled together, (2.8) and (2.9) provide a closed system. Also, p_2 can be replaced in (2.9) by its limiting value $p_{2\infty}(t_m, x_m, z_m)$, as $y_2\to\infty$, because the change in pressure across the main deck is $O(\varepsilon)$ because of (2.8). Thus, the normal velocity is obtainable first from (2.9) independent of the pressure, then integrating (2.8) gives an expression for the pressure. This asymptotically valid procedure is used as a basis in the following sections. Note also that (2.9) essentially simplifies on passing to the limit of incompressible fluid as $M_\infty\to 0$. On the other hand, the possibility for a critical layer to be embedded in the main deck is completely ignored with $p_{2\infty}$ substituted for p_2 in (2.9). This implies that disturbances of the travelling wave type are supposed to propagate within the near-wall sublayer. To meet the latter constraint the phase velocity of disturbances must be $O(\varepsilon)$ or less.

In the near-wall viscous sublayer we employ again the stretched independent variables t, x, z defined in (2.1*a, b*) and introduce the normal coordinate

$$y'=\varepsilon^5\tau_w^{-3/4}C^{5/8}\left(T_w^*/T_\infty^*\right)^{3/2}y_3. \tag{2.10}$$

The velocity components are scaled and normalized here by means of

$$(u',w')=\varepsilon\tau_w^{1/4}C^{1/8}(T_w^*/T_\infty^*)^{1/2}(u_3,w_3), \tag{2.11a}$$

$$v'=\varepsilon^3\tau_w^{3/4}C^{3/8}(T_w^*/T_\infty)^{1/2}v_3, \tag{2.11b}$$

whereas the density $\rho'=R_0(0)=(T_w^*/T_\infty^*)^{-1}$ is held constant and the pressure p' takes on the same form as in (2.3). Upon substituting (2.1*a, b*), (2.10), (2.11*a, b*) and aforementioned expressions for ρ' and p' into the initial Navier–Stokes equations we arrive at a system of Prandtl equations

$$\frac{\partial u_3}{\partial x}+\frac{\partial v_3}{\partial y_3}+\frac{\partial w_3}{\partial z}=0, \tag{2.12a}$$

$$\frac{\partial u_3}{\partial t}+u_3\frac{\partial u_3}{\partial x}+v_3\frac{\partial u_3}{\partial y_3}+w_3\frac{\partial u_3}{\partial z}=-\frac{\partial p_3}{\partial x}+\frac{\partial^2 u_3}{\partial y_3^2}, \tag{2.12b}$$

$$\frac{\partial w_3}{\partial t}+u_3\frac{\partial w_3}{\partial x}+v_3\frac{\partial w_3}{\partial y_3}+w_3\frac{\partial w_3}{\partial z}=-\frac{\partial p_3}{\partial z}+\frac{\partial^2 w_3}{\partial y_3^2}, \tag{2.12c}$$

for an incompressible boundary layer where both components $\partial p_3/\partial x$ and $\partial p_3/\partial z$ of the pressure gradient in a plane parallel to the flat solid surface are to be evaluated simultaneously with the velocity field. Since the pressure variations across the near-wall sublayer turn out to be $O(\varepsilon^4)$ we put $\partial p_3/\partial y_3 = 0$, in keeping with the conventional version of the triple deck. Accordingly, no additional higher-order terms depending on the small parameter ε enter (2.12*a*–*c*), so we can use pertinent results set forth in Stewart & Smith (1987)and Ryzhov & Terent'ev (1991).

Solutions to systems of equations (2.8), (2.9) and (2.12*a*–*c*) for the main deck and the lower near-wall sublayer, respectively, are to be developed subject to matching conditions which will be discussed in some detail below. Besides, (2.6) needs to be taken into account through the matching with a solution for the main deck. The no-slip conditions $u_3 = v_3 = w_3 = 0$ hold at the flat surface $y_3 = 0$.

3. Linear approximation

The velocity components $U_{xo}(y_2)$ and $U_{zo}(y_2)$ of the initially steady three-dimensional boundary layer in the vicinity of a wall, as $y_2 \to 0$, are $U_{xo} = y_2 \mathrm{d}U_{xo}(0)/\mathrm{d}y_2$ and $U_{zo} = y_2 \mathrm{d}U_{zo}(0)/\mathrm{d}y_2$ to leading order. Thus, following the traditional theory of hydrodynamic stability we may write

$$(u_3-\tau_x y_3, v_3, w_3-\tau_z y_3, p_3) = a\,[\tau_x f(y_3), g(y_3), \tau_z h(y_3), p_{30}]\exp[\mathrm{i}(\omega t+kx+mz)] \tag{3.1}$$

with allowance made for the definition of τ_x and τ_z in (1.1*a, b*). On the assumption that a value of the travelling wave amplitude a is indefinitely small, substitution of (3.1) into the system of the Prandtl equations yields

$$\frac{\mathrm{d}g}{\mathrm{d}y_3}=-\mathrm{i}(k\tau_x f+m\tau_z h), \tag{3.2a}$$

$$\frac{\mathrm{d}^2 f}{\mathrm{d}y_3^2}=\mathrm{i}(\omega+k\tau_x y_3+m\tau_z y_3)f+g+\frac{\mathrm{i}k}{\tau_x}p_{30}, \tag{3.2b}$$

$$\frac{\mathrm{d}^2 h}{\mathrm{d}y_3^2}=\mathrm{i}(\omega+k\tau_x y_3+m\tau_z y_3)h+g+\frac{\mathrm{i}m}{\tau_z}p_{30}. \tag{3.2c}$$

Let us consider a reduced wavenumber $K = k\tau_x + m\tau_z$ and a function $F = k\tau_x f + m\tau_z h$. Upon differentiating (3.2*b*), (3.2*c*) and eliminating $\mathrm{d}g/\mathrm{d}y_3$ between the resulting expressions and (3.2*a*) we obtain

$$\frac{\mathrm{d}^3 F}{\mathrm{d}y_3^3}-\mathrm{i}(\omega+Ky_3)\frac{\mathrm{d}F}{\mathrm{d}y_3}=0. \tag{3.3}$$

Precisely the same equation controls the propagation of TS waves in a Blasius boundary layer with parameters independent of z. This property is the essence of a transformation by Squire (1933) which remains valid asymptotically, as $\varepsilon \to 0$, even if a steady three-dimensional motion of a compressible fluid involves the crossflow in the local spanwise direction.

Two constraints to be imposed on a desired solution of (3.3) at the solid surface come from the no-slip conditions $f = g = h = 0$ and an appropriate linear combination of (3.2*b*) and (3.2*c*); they are

$$F = 0, \quad \frac{d^2F}{dy_3^2} = i(k^2 + m^2)p_{30} \quad \text{at} \quad y_3 = 0. \tag{3.4}$$

The standard technique (see for example Ryzhov & Terent'ev 1986) which is based on introducing a new independent variable $Y = \Omega + i^{1/3}K^{1/3}y_3$, $\Omega = i^{1/3}\omega K^{-2/3}$ can be used to analyse (3.3). It should be mentioned that a cut along the positive imaginary semi-axis is drawn in the complex K-plane which defines a single-valued branch of the function $K^{1/3}$ by means of $-3\pi/2 < \arg(K) < \pi/2$. As a result we have

$$\frac{dF}{dY} = \frac{i^{1/3}(k^2 + m^2)p_{30}}{K^{2/3}} \left[\frac{d\mathrm{Ai}(\Omega)}{dY}\right]^{-1} \mathrm{Ai}(Y) \tag{3.5}$$

where $\mathrm{Ai}(Y)$ denotes an Airy function. In addition to (3.4) we need two more constraints to evaluate the constant p_{30} and specify the limiting condition for F at the outer reaches, as $y_3 \to \infty$, of the near-wall sublayer. Both of them are obtainable from the matching of (2.6) with the disturbance field in most of the boundary layer.

In the upper deck, a solution of travelling wave type that corresponds to (3.1) reads

$$\varphi_1 = a\varphi_{10} \exp[i(\omega t + kx + mz) - \ell y_1], \tag{3.6a}$$

$$\ell = \left[\left(1 - M_\infty^2\right)k^2 + m^2\right]^{1/2}. \tag{3.6b}$$

The square root on the right-hand side of (3.6*b*) is meant to be positive for all real (positive as well as negative) values of k and m provided that $M_\infty < 1$. Applying (3.6*a*) to (2.6) taken at $y_1 = 0$ results in

$$p_1 = ap_{10} \exp[i(\omega t + kx + mz) - \ell y_1], \quad p_{10} = -ik\varphi_{10}. \tag{3.7}$$

In what follows it is preferable to deal with the constant p_{10} rather than φ_{10}.

In the main deck we put

$$(u_2, v_2, w_2, \rho_2, p_2) = a\,[f_2(y_2), g_2(y_2), h_2(y_2), \hat{\rho}_2(y_2), \hat{p}_2(y_2)] \exp[i(\hat{\omega}t_m + \hat{k}x_m + \hat{m}z_m)] \tag{3.8}$$

where the frequency $\hat{\omega}$ and wavenumbers $\hat{k}$, $\hat{m}$ in unstretched variables t_m, x_m, z_m are expressed in terms of ω and k, m through

$$\hat{\omega} = \tau^{3/2}C^{-1/4}(T_w^*/T_\infty^*)^{-1}\omega, \quad (\hat{k}, \hat{m}) = \tau^{5/4}C^{-3/8}(T_w^*/T_\infty^*)^{-3/2}(k, m). \tag{3.9}$$

As has been explained above, p_2 can to leading order be replaced in (2.9) by its limiting value $p_{2\infty}(t_m, x_m, z_m)$, as $y_2 \to \infty$. Introducing then (3.8) into (2.9) we arrive at the simple equation

$$\frac{dg_2}{dy_2} - \frac{\hat{k}dU_{xo}/dy_2 + \hat{m}dU_{zo}/dy_2}{\hat{k}U_{xo} + \hat{m}U_{zo}}g_2 + i\varepsilon\hat{p}_{2\infty}\left[M_\infty^2\left(\hat{k}U_{xo} + \hat{m}U_{zo}\right) - \frac{\hat{k}^2 + \hat{m}^2}{R_0(\hat{k}U_{xo} + \hat{m}U_{zo})}\right] = 0 \tag{3.10}$$

whose solution has to be matched, as $y_2 \to \infty$ and $y_1 \to 0$, to an expression ensuing from the definition $v_1 = \partial\varphi_1/\partial y_1$ of the vertical velocity in the upper sublayer. Upon matching, the solution of (3.10) becomes

$$g_2 = \tau_w^{1/2} C^{1/4} \mathrm{i} p_{10} \left(\hat{k} U_{xo} + \hat{m} U_{zo}\right) \left\{ -\frac{\hat{\ell}}{\hat{k}^2} + \varepsilon \frac{\hat{\ell}^2}{\hat{k}^2} y_2 + \varepsilon(\hat{k}^2 + \hat{m}^2) \int_{y_2}^{\infty} \left[\frac{1}{\hat{k}^2} - \frac{1}{R_0 (\hat{k} U_{xo} + \hat{m} U_{zo})^2} \right] \mathrm{d}y_2 \right\}, \tag{3.11a}$$

$$\hat{\ell} = \left[\left(1 - M_\infty^2\right) \hat{k}^2 + \hat{m}^2 \right]^{1/2} = \tau_w^{5/4} C^{-3/8} (T_w^* / T_\infty^*)^{-3/2} \ell. \tag{3.11b}$$

With a relationship for g_2 to hand, we integrate an equation for $\hat{p}_2$ which derives from (2.8) provided that a class of travelling waves (3.8) is under consideration. The result of integration can be cast in the form

$$\hat{p}_2 = \hat{p}_{20} - \varepsilon \tau_w^{1/2} C^{1/4} p_{10} \hat{\ell} y_2 - \mathrm{i}\varepsilon \hat{k} \int_0^{y_2} \left(R_0 U_{xo} g_2 + \tau_w^{1/2} C^{1/4} \frac{\mathrm{i} p_{10} \hat{\ell}}{\hat{k}} \right) \mathrm{d}y_2 - \mathrm{i}\varepsilon \hat{m} \int_0^{y_2} R_0 U_{zo} g_2 \mathrm{d}y_2 \tag{3.12}$$

where $\hat{p}_{20} = \hat{p}_2(0)$. A value of $\hat{p}_{20}$ comes from the two-term matching of (3.12) with g_2 given by (3.11*a*) in the limit as $y_2 \to \infty$ to the corresponding expansion of (3.7) evaluated as $y_1 \to 0$. The final result reads

$$\hat{p}_{20} = \tau_w^{1/2} C^{1/4} \frac{p_{10} \hat{\ell}}{\hat{k}^2} \left[\frac{\hat{k}^2}{\hat{\ell}} - \varepsilon \hat{k}^2 D_{(xx)} + 2\varepsilon \hat{k} \hat{m} D_{(xz)} + \varepsilon \hat{m}^2 D_{(zz)} \right] \tag{3.13}$$

with all the integrals

$$D_{(xx)} = \int_0^\infty (1 - R_0 U_{xo}^2) \mathrm{d}y_2, \tag{3.14a}$$

$$D_{(xz)} = \int_0^\infty R_0 U_{xo} U_{zo} \mathrm{d}y_2, \tag{3.14b}$$

$$D_{(zz)} = \int_0^\infty R_0 U_{zo}^2 \mathrm{d}y_2, \tag{3.14c}$$

being independent of the frequency $\hat{\omega}$ and wavenumbers $\hat{k}$, $\hat{m}$ of travelling waves. According to (3.14*a–c*), $D_{(xx)}$, $D_{(xz)}$, $D_{(zz)}$ are the instanteneous momentum thicknesses of the boundary layer. In terms of g_2 and $\hat{p}_{20}$ the horizontal velocities can be expressed as

$$f_2 = \mathrm{i} \frac{\mathrm{d}U_{xo}}{\mathrm{d}y_2} \frac{g_2}{\hat{k} U_{xo} + \hat{m} U_{zo}} - \frac{\varepsilon \hat{k}}{R_0} \frac{\hat{p}_{20}}{\hat{k} U_{xo} + \hat{m} U_{zo}}, \tag{3.15a}$$

$$h_2 = \mathrm{i} \frac{\mathrm{d}U_{zo}}{\mathrm{d}y_2} \frac{g_2}{\hat{k} U_{xo} + \hat{m} U_{zo}} - \frac{\varepsilon \hat{m}}{R_0} \frac{\hat{p}_{20}}{\hat{k} U_{xo} + \hat{m} U_{zo}}. \tag{3.15b}$$

We are now in a position to write down the first required constraint

$$p_{30} = \tau_w^{-1/2} C^{-1/4} \hat{p}_{20}(p_{10}, \hat{k}, \hat{m}) \tag{3.16}$$

with $\hat{p}_{20}$ depending on p_{10} and also $\hat{k}, \hat{m}$ through (3.13). With allowance made for

(3.16) integrating (3.5) yields

$$\Phi(\Omega) = \tau_w^{-1/2} C^{-1/4} \frac{\mathrm{i}^{1/3}(k^2+m^2)}{K^{2/3}} \frac{\hat{p}_{20}}{F(\infty)}, \tag{3.17a}$$

$$\Phi(\Omega) = \frac{\mathrm{dAi}(\Omega)}{\mathrm{d}Y} \left[\int_{\Omega}^{\infty} \mathrm{Ai}(Y)\mathrm{d}Y \right]^{-1} \tag{3.17b}$$

where $\hat{k}, \hat{m}$ and $\hat{\ell}$ involved in $\hat{p}_{20}$ are replaced by k, m, and ℓ using (3.9) and (3.11*b*), respectively. The ratio $\hat{p}_{20}/F(\infty)$ entering the right-hand side of (3.17*a*) is to be found from matching a linear combination $k\tau_x f_2 + m\tau_z g_2$ defined by means of (3.15*a, b*) with F, as $y_2 \to 0$ and $y_3 \to \infty$. This final step results in a dispersion relation connecting the frequency ω of eigenmodes with their two wavenumbers k and m. However, before we set about analysing the dispersion relation for finite values of ε, let us consider its properties in the limit as $\varepsilon \to 0$.

4. Classical triple-deck approach

If $\varepsilon = 0$ a relationship

$$\lim_{y_2 \to 0} \frac{g_2}{\hat{k}U_{xo} + \hat{m}U_{zo}} = -\mathrm{i}\tau_w^{1/2} C^{1/4} \frac{\hat{\ell}}{\hat{k}^2} p_{10} \tag{4.1}$$

is obtainable from (3.11*a*). With (4.1) accounted for, (3.15*a, b*) reduce to

$$f_2(0) = \tau_w^{1/2} C^{1/4} \frac{\mathrm{d}U_{xo}(0)}{\mathrm{d}y_2} \frac{\hat{\ell}}{\hat{k}^2} p_{10}, \quad h_2(0) = \tau_w^{1/2} C^{1/4} \frac{\mathrm{d}U_{zo}(0)}{\mathrm{d}y_2} \frac{\hat{\ell}}{\hat{k}^2} p_{10}. \tag{4.2a, b}$$

Upon substituting the normalized wall shear stresses τ_x and τ_z defined by (1.1*a, b*) for $\mathrm{d}U_{xo}(0)/\mathrm{d}y_2$ and $\mathrm{d}U_{zo}(0)/\mathrm{d}y_2$ in (4.2*a, b*), respectively, the second desired condition takes the simple form

$$F(\infty) = \frac{\ell K}{k^2} p_{10}, \tag{4.3}$$

where $K = k\tau_x + m\tau_z$. Insofar as $\hat{p}_{20} = \tau_w^{1/2} C^{1/4} p_{10}$ in the classical triple-deck approach we arrive at the following dispersion relation (Manuilovich 1983; Stewart & Smith 1987; Ryzhov & Terent'ev 1991):

$$\Phi(\Omega) = \frac{\mathrm{i}^{1/3} k^2 (k^2+m^2)}{\left[(1-M_\infty^2)k^2 + m^2\right]^{1/2} K^{5/3}}. \tag{4.4}$$

Here the square root of $(1-M_\infty^2)k^2 + m^2$ is meant to be positive for all real values of k and m. By virtue of (3.17*b*), Φ has an explicit expression in terms of a derivative and improper integral of the Airy function depending on a single argument Ω that makes mapping (4.4) onto the complex Ω-plane particularly illuminative when analysing the dispersion-relation properties. All the singular points in the Ω-plane are known from Ryzhov & Terent'ev (1986, 1991) whose results are used as guidelines below.

Let k and m be real and positive. On the strength of a constraint $-3\pi/2 < \arg(K) < \pi/2$ imposed on values of K in §3, we write $-k$ and $-m$ as $\mathrm{e}^{-\mathrm{i}\pi}k$ and $\mathrm{e}^{-\mathrm{i}\pi}m$, respectively. Suppose that three numbers ω, k, m with ω being complex satisfy (4.4). Then the other three numbers $-\omega_{c.c.}$,$-k$,$-m$, where a subscript *c.c.* denotes the appropriate complex conjugate, also form a solution to (4.4). This statement

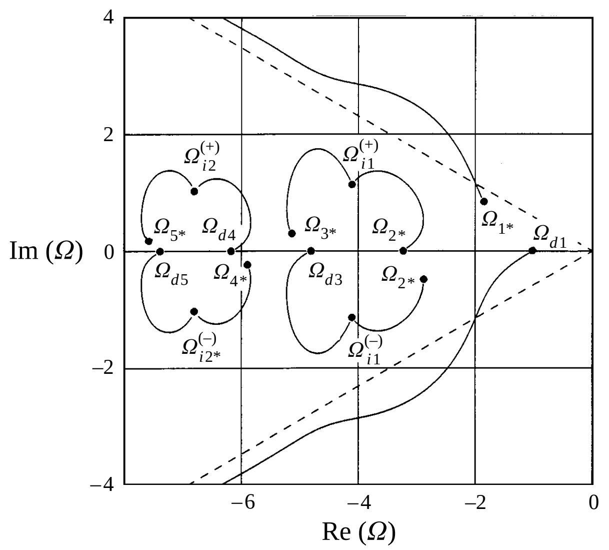

FIGURE 2. Trajectories of the dispersion-relation roots in the complex Ω-plane made by image points with both wavenumber k, m taking real values. The points Ω_{dj} on the real negative semi-axis are zeros of $\mathrm{dAi}(\Omega)/\mathrm{d}Y$; the complex conjugate pairs $\Omega_{Ij}^{(\pm)}$ are defined by an equation $\int_{\Omega}^{\infty} \mathrm{Ai}(Y)\mathrm{d}Y = 0$; the limiting points Ω_{j*} for $m > 0$ are fixed by sharp turns in the motion of image points along trajectories; $j = 1, 2, \ldots$.

immediately follows from the definition

$$\Omega(-\omega_{c.c.}, -k, -m) = -\mathrm{i}^{1/3}\omega_{c.c.}(-k\tau_x - m\tau_z)^{-2/3} = \Omega_{c.c.} \tag{4.5}$$

of Ω and symmetry properties of the Airy function leading to the simple result

$$\Phi(\Omega_{c.c.}) = \Phi(\Omega)_{c.c.}. \tag{4.6}$$

With k and m fixed, the dispersion-relation roots form a countable set of image points in the Ω-plane. When k and m vary taking on real values these points move along certain trajectories which constitute a collection of dispersion curves. It is worthy of note that each of the image points may proceed in both directions along its own dispersion curve even if k and m monotonically increase or decrease. As (3.17b) shows, in the limit $k \to 0$, all the points under consideration approach the real negative semi-axis and tend to those points which are determined by the roots Ω_{dj} of an equation $\mathrm{dAi}(\Omega_{dj})/\mathrm{d}Y = 0$. Accordingly, the dispersion curves $\Omega_j = \Omega_j(k, m; \tau_x, \tau_z, M_\infty)$ may be arranged in ascending order by labelling them with zeros of $\mathrm{dAi}(\Omega_{dj})/\mathrm{d}Y$. Figure 2 presents a typical plot of the Ω-plane. The first dispersion curve arising from Ω_{d1} extends to infinity. All of the dispersion curves with origins at Ω_{dj}, $j = 2, 3, \ldots$, extend to the points $\Omega_{Ij}^{(\pm)}$ fixed by means of the complex conjugate roots of an equation $I(\Omega_{Ij}^{(\pm)}) = 0$ where $I(\Omega)$ is an improper integral $\int_{\Omega}^{\infty} \mathrm{Ai}(Y)\mathrm{d}Y$ entering the right-hand side of (3.17b).

The dispersion curves in figure 2 are identical with those obtainable from the asymptotic analysis of normal ($m = 0$) TS waves propagating in a Blasius boundary layer with $\tau_x > 0$ and $\tau_z = 0$ (Ryzhov & Terent'ev 1986). However, in the general three-dimensional case of interest the spanwise component τ_z of the wall shear stress differs from zero and, besides, the spanwise wavenumber m does not vanish (to be specific we assume that both $\tau_x > 0$ and $\tau_z > 0$ in keeping with figure 1). Non-trivial values of τ_z give rise to important distinctions featuring the image-point motion along each of the dispersion curves in the Ω-plane when passing from a two-dimensional consideration to the general study of eigenmodes in a three-dimensional boundary layer. Our concern is primarily with the first dispersion curve since it relates to self-excited oscillations; all the other curves lead to exponentially damped disturbances. Recall that steady vortices stretching in the local streamwise direction are at the heart of crossflow instability: in this case the two wavenumbers k and m are connected through the dispersion relation (4.4) with $\Omega = 0$. So, the origin of the coordinates is a degenerate map of steady vortical disturbances onto the Ω-plane, and they need to be studied separately (see Stewart & Smith 1987).

We consider in more detail the image-point motion along the first dispersion curve Ω_1 with the condition that the streamwise wavenumber k takes negative and positive values whereas $m = m_0 = \text{const}$. The asymptotic behaviour of Ω_1, as $k \to -\infty$, follows from

$$\Omega_1 \to \infty \exp(5\pi i/6). \tag{4.7}$$

An increase in k leads to downward motion along the curve to a certain limiting point Ω_{1*} whose position is dependent on the sign of m_0. Let $m_0 > 0$, then Ω_{1*} is located as shown in figure 2, i.e. in the upper half-plane of the complex Ω-plane. Precise values of $\text{Re}(\Omega_{1*})$ and $\text{Im}(\Omega_{1*})$ are determined by m_0 and the three parameters τ_x, τ_z and M_∞. Upon reaching the limiting point the motion along the first dispersion curve changes to the opposite direction and the image point starts climbing upwards; as a result (4.7) comes into operation, as $K \to -0$ and $k \to -m_0\tau_z/\tau_x$. The passage through $K = 0$ is marked by a sudden jump of the image point onto a branch of the dispersion curve located in the lower half-plane of the Ω-plane, the corresponding asymptotics being

$$\Omega_1 \to \infty \exp(-5\pi i/6), \tag{4.8}$$

as $K \to +0$. It is evident that the first zero Ω_{d1} of the derivative of the Airy function is a limiting point in the motion along the lower branch of the first dispersion curve; it is attained when $k = 0$. Upon reaching Ω_{d1} and making a sharp upward turn here the image point proceeds along the same branch in the opposite direction to complete its motion with the asymptote (4.8), as $k \to \infty$.

The question of how the first dispersion curve is used to describe the image-point motion provided that $m_0 < 0$ can be readily settled using the symmetry properties (4.5) and (4.6). A change in the direction of the motion along a branch of this curve in the upper half-plane takes place at the point Ω_{d1} when $k = 0$. The subsequent passage through $K = 0$ entails a sudden jump onto another branch of the dispersion curve which lies in the lower half-plane. The image point moves upwards to a limiting point Ω_{1*} in this half-plane where makes a sharp turn to descend finally. An important feature is that the points Ω_{1*} and Ω_{d1} are separated by a finite distance if $m_0 \neq 0$. However, $K = k\tau_x$ with $m_0 = 0$, in which case (4.4) reduces to a dispersion relation controlling normal TS waves in an incompressible Blasius boundary layer. As a result, Ω_{1*} and Ω_{d1} merge to form a double point, ruling out the possibility for a sharp turn to occur at $k = 0$. The situation is similar with regard to the image-point motion along all the other dispersion curves in figure 2. The only difference is that $\Omega_j \to \Omega_{Ij}^{(\pm)}$, $j = 2, 3, \ldots$, as $k \to \pm\infty$.

The eigenmode growth or decay depends on $\arg(\omega)$ of the complex frequency ω. On the other hand, $\arg(K)$ can be equal to 0 or $-\pi$ when both wavenumbers k and m take on real values. Since the disturbance amplitude exponentially increases in the range $-\pi < \arg(\omega) < 0$, a domain of self-excited oscillations is defined in the Ω-plane by conditions

$$-5\pi/6 < \arg(\Omega) < \pi/6 \quad \text{if} \quad \arg(K) = 0, \tag{4.9a}$$

$$-\pi/6 < \arg(\Omega) < 5\pi/6 \quad \text{if} \quad \arg(K) = -\pi. \tag{4.9b}$$

Inclination angles of rays shown in figure 2 by the dashed lines are fixed by $\arg(\Omega) = 5\pi/6$ and $\arg(\Omega) = -5\pi/6$. The rays intersect only the first dispersion curve with the same slope $\Omega_1 \sim \infty \exp(\pm 5\pi i/6)$ at infinity as given in (4.7) and (4.8). So, there exists a range of real values of k and m to meet the constraints (4.9*a, b*). Accordingly, the first root of the dispersion relation specifies the frequency and two wavenumbers of unstable eigenmodes in this range. All the other roots relate to disturbances with the amplitude exponentially vanishing with time. One may observe that the analysis of stability properties in the complex Ω-plane as applied to three-dimensional boundary layers follows along the lines of the corresponding study by Ryzhov & Terent'ev (1986) of normal TS waves in a Blasius boundary layer. The sole distinction comes from the occurrence of a limiting point Ω_{1*} which results in the image-point motion in both directions along the same curve. In addition, the dispersion curves in the Ω-plane are of standard shape, therefore advantage may be taken of the foregoing consideration when examining alternative problems on shear-flow stability.

The first singularity in solutions to the dispersion relation comes from the passage of the reduced wavenumber K through zero with k and m taking on finite values k_0 and m_0, respectively. The apparent meaning of $K = k_0\tau_z + m_0\tau_z = 0$ is that the wave vector is orthogonal to the direction of the wall shear stress. By virtue of (4.4) we arrive in the limit $K \to 0$ at the following asymptotic representation:

$$\omega_1 \sim -\frac{c_0^2}{K} - \frac{\sqrt{2}}{2}(1+i)\frac{K^3}{c_0} + \dots, \quad c_0^2 = \frac{k_0^2(k_0^2+m_0^2)}{\left[(1-M_\infty^2)k_0^2+m_0^2\right]^{1/2}}, \tag{4.10a, b}$$

where ω_1 implies the first root of ω. In spite of the fact that a singularity enters $\mathrm{Re}(\omega_1)$, the Cauchy problem remains well posed in a linear approximation for $\mathrm{Im}(\omega_1) = -\sqrt{2}K^3/(2c_0) \to 0$ in (4.10*a, b*), as $K \to 0$. An analogous singularity turns out to also be intrinsic to unsteady Görtler vortices in an incompressible boundary layer on a curved surface (see Ruban 1990, Savenkov 1990 and critisisms by Choudhari, Hall & Streett 1994).

The second, and much stronger, singularity stems from non-monotonic behaviour of ω_1 as a function of both wavenumbers. In order to derive this singularity let us first tackle the issue on level lines of $\mathrm{Im}(\omega_1)$ using results found above in the Ω-plane on the assumption that k and m are real. The contours are shown in figure 3 for a boundary layer with $M_\infty = 0.2, \tau_x = \sqrt{8}/3$ and $\tau_z = 1/3$, the symmetry properties (4.5), (4.6) being clearly recognizable in their shapes. Therefore, we may restrict ourselves to inspection of the first and the second quadrants of the (k, m)-plane.

It is advisable to put $m = ck^3$ with $c > 0$ and let $k \to \infty$ for elucidating the properties of the disturbance amplitude amplification rate which are specified by curves in the first quadrant. Then (4.4) yields

$$\Phi(\Omega) = i^{1/3}c^{-2/3}\tau_z^{-5/3}, \tag{4.11}$$

to leading order, with the right-hand side being independent of k and m. The magnitude of the frequency ensuing from (4.11) is

$$\omega = i^{-1/3}\Omega\, c^{2/3}\tau_z^{2/3}k^2. \tag{4.12}$$

An important conclusion can be drawn from a comparison of (4.11) with a dispersion

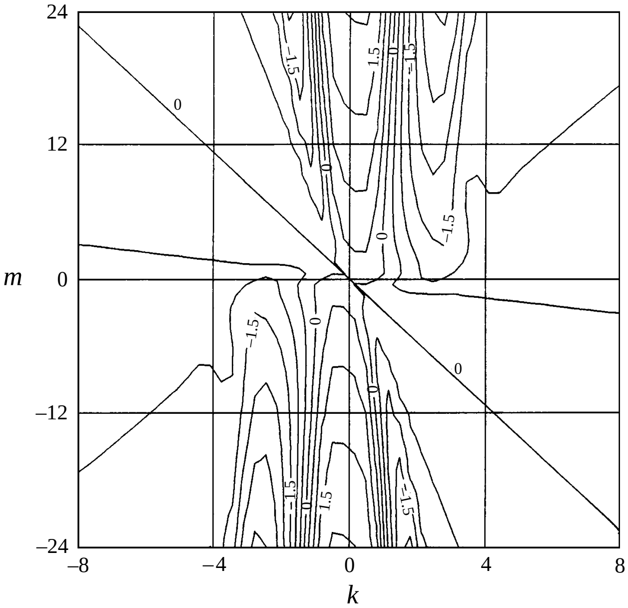

FIGURE 3. Contours of $\mathrm{Im}(\omega_1)$ in the real (k, m)-plane formed by both wavenumbers within the framework of the classical triple-deck theory; $\varepsilon = 0, M_\infty = 0.2, \tau_x = \sqrt{8}/3, \tau_z = 1/3$.

relation controlling normal ($m = 0$) TS waves in an incompressible boundary layer where the spanwise skin friction $\tau_z = 0$. In the latter case the disturbance amplitude remains constant in time if the streamwise wavenumber $k = k_* = 1.0005$. It follows that a constant $c = c_* = k_*^{-2}\tau_z^{-5/2} = 0.999\tau_z^{-5/2}$ determines the asymptotics of neutral oscillations in a subsonic boundary layer, whatever value of $M_\infty < 1$ is under consideration. The frequency $\omega = \omega_*$ of neutral oscillations is fixed by (4.12). An analogous statement holds for the third quadrant of the (k, m)-plane where $k \to -\infty$.

Thus, the curve $m = c_* k^3$ is an asymptote to separate self-excited eigenmodes given by $c < c_*$ from stable waves with $c > c_*$. Furthermore, among self-excited eigenmodes in a Blasius boundary layer we may isolate disturbances whose amplitude amplification rate attains extremal values. The corresponding streamwise wavenumbers of normal ($m = 0$) TS waves are defined as $k = k_2^* = 2.716, k = k_4^* = 4.346$ for two maxima and $k = k_3^* = 3.616$ for a minimum in between (Ryzhov & Terent'ev 1986; Smith 1989). It is obvious that the constants $c = c_2^* = (k_2^*)^{-2}\tau_z^{-5/2} = 0.1356\tau_z^{-5/2}$, $c = c_3^* = (k_3)^{-2}\tau_z^{-5/2} = 0.07648\tau_z^{-5/2}$ and $c = c_4^* = (k_4^*)^{-2}\tau_z^{-5/2} = 0.05294\tau_z^{-5/2}$ possess analogous extremal properties in the present analysis of short-scaled three-dimensional disturbances governed by (4.11). In fact, with allowance made for (4.12) we obtain solutions for Ω_1 with two local negative minima $\mathrm{Im}\left[\mathrm{i}^{-1/3}\Omega_{12}^*(c_2^*)^{2/3}\tau_z^{2/3}\right]$, $\mathrm{Im}\left[\mathrm{i}^{-1/3}\Omega_{14}^*(c_4^*)^{2/3}\tau_z^{2/3}\right]$ and a local negative maximum $\mathrm{Im}\left[\mathrm{i}^{-1/3}\Omega_{13}^*(c_3^*)^{2/3}\tau_z^{2/3}\right]$ of a ratio $\mathrm{Im}(\omega_1/k^2)$. A domain around the major local minimum $\mathrm{Im}\left[\mathrm{i}^{-1/3}\Omega_{12}^*(c_2^*)^{2/3}\tau_z^{2/3}\right]$ is clearly discernible in figure 3, some wiggles in contours of $\mathrm{Im}(\omega_1)$ are provoked by the local maximum $\mathrm{Im}\left[\mathrm{i}^{-1/3}\Omega_{13}^*(c_3^*)^{2/3}\tau_z^{2/3}\right]$ and the second, less-marked minimum $\mathrm{Im}\left[\mathrm{i}^{-1/3}\Omega_{14}^*(c_4^*)^{2/3}\tau_z^{2/3}\right]$. In keeping with the aforementioned papers by Ryzhov &

Terent'ev (1986) and Smith (1989) the double-mound shape of the growth-rate dependence on both wavenumbers dominates the instability of normal ($m = 0$) TS waves. Moreover, the amplitude amplification rate of self-excited eigenmodes with $c < c_*$ inherent in the three-dimensional boundary layer is estimated by $\mathrm{Im}(\omega_1) \sim -k^2 \to -\infty$ in the limit as $k \to \infty$. The occurrence of this singularity is of conceptual importance since the Cauchy problem turns out to be ill posed in the framework of a linear version of the triple-deck theory.

We may arrive at the same conclusion that the Cauchy problem for a system of linear equations is ill posed by considering the second quadrant of the (k, m)-plane shown in figure 3 (the contours of $\mathrm{Im}(\omega_1)$ in the fourth quadrant are similar in shape). Let $k \to -\infty$ under conditions that $m = ck^3$ and $c < 0$. Since the reduced wavenumber $K > 0$ in view of $m > 0$, (4.11) and (4.12) still remain valid if c is replaced by $|c|$. It follows from the foregoing that a curve $m = -c_* k^3$ with $c_* = 0.999\tau_z^{-5/2}$ is the second branch of the asymptote which separates self-excited eigenmodes from stable waves with exponentially vanishing amplitude. To the left of this branch a domain stands out sharply whose existence is brought about by the major local minimum $\mathrm{Im}\left[\mathrm{i}^{-1/3}\Omega_{12}^*(c_2^*)^{2/3}\tau_z^{2/3}\right]$; wiggles in the contours of $\mathrm{Im}(\omega_1)$ attributable to the local maximum $\mathrm{Im}\left[\mathrm{i}^{-1/3}\Omega_{13}^*(c_3^*)^{2/3}\tau_z^{2/3}\right]$ and the second, weaker minimum $\mathrm{Im}\left[\mathrm{i}^{-1/3}\Omega_{14}^*(c_4^*)^{2/3}\tau_z^{2/3}\right]$ are hardly discernible. From a conceptual point of view, the most important result is that the growth rate of self-excited eigenmodes with $|c| < c_*$ complies with an estimate $\mathrm{Im}(\omega_1) \sim -k^2 \to -\infty$ in the limit as $k \to -\infty$.

5. Short-scaled eigenmodes

We omit an in-depth analysis of high-frequency disturbances of finite wavelength which obey (4.10a, b) because the corresponding singularity does not lead to ill-posedness of the Cauchy problem. It will suffice to mention that in this case ω_1 tends to $O(\varepsilon^{-1})$ from (3.7), (3.11a, b) or (3.13). On the other hand, the second, and much stronger, singularity arising from the assumption that $m = ck^3$, as $|k| \to \infty$, requires a careful treatment calling into question the very validity of the triple-deck model as applied to three-dimensional boundary layers.

The simplest way to derive new scalings of the eigenmode frequency and wavenumbers in the limiting case under consideration is to compare the leading term k^2/ℓ with the main correction term $\varepsilon m^2 D_{(zz)}$ in square brackets on the right-hand side of (3.13). If $\ell \sim m$ we have $k^2 \sim \varepsilon m^3$ with the final result $k \sim \varepsilon^{-1/7}$, $m \sim \varepsilon^{-3/7}$ ensuing from the fact that $m \sim k^3$. The corresponding calibration of the frequency is $\omega \sim k^2 \sim \varepsilon^{-2/7}$. Then, the position of a critical layer may be estimated through $\varepsilon\omega \sim mU_{zo}(y_2)$, as $y_2 \to 0$, whence

$$y_2 \sim \varepsilon k^{-1} \sim \varepsilon^{8/7}. \tag{5.1}$$

Scalings based on a comparison of the leading term k^2/ℓ with terms $\varepsilon kmD_{(xz)}$ and $\varepsilon k^2 D_{(xx)}$ entering (3.13) would be $k \sim \varepsilon^{-1/5}$ and $k \sim \varepsilon^{-1/3}$, respectively. They relate to eigenmodes with much shorter wavelengths.

With calibration of the frequency and both wavenumbers in hand, we may introduce new independent variables

$$t' = \varepsilon^{16/7}\tilde{t} = R^{-2/7}\tilde{t}, \tag{5.2a}$$

$$x' = \varepsilon^{22/7}\tilde{x} = R^{-11/28}\tilde{x}, \quad y' = \varepsilon^4 y_2 = R^{-1/2}y_2, \quad z' = \varepsilon^{24/7}\tilde{z} = R^{-3/7}\tilde{z} \quad (5.2b\text{–}d)$$

for most of the boundary layer when examining disturbances slightly elongated in the local streamwise direction. The desired functions in this sublayer are sought in the form of asymptotic sequences

$$[u' - U_{xo}(y_2), \quad w' - U_{zo}(y_2), \quad \rho' - R_0(y_2)] = \varepsilon^{8/7} (\tilde{u}_2, \tilde{w}_2, \tilde{\rho}_2) = R^{-1/7} (\tilde{u}_2, \tilde{w}_2, \tilde{\rho}_2), \tag{5.3a, b}$$

$$v' = \varepsilon^{12/7} \tilde{v}_2 = R^{-3/14} \tilde{v}_2, \quad p' = \varepsilon^{16/7} \tilde{p}_2 = R^{-2/7} \tilde{p}_2 \tag{5.3c, d}$$

From substitution of (5.2*a*–*d*) and (5.3*a*–*d*) into the original Navier–Stokes equations we may conclude that of the two second-order terms on the left-hand side of (2.8) only the last one should be retained, giving rise to a non-vanishing component of the pressure gradient in a direction normal to the solid surface. The term with the spatial derivative of v_2 with respect to x_m becomes negligible. A solution to the resulting system of asymptotic equations related to new variables reads

$$\tilde{u}_2 = \tilde{A}(\tilde{t}, \tilde{x}, \tilde{z}) \frac{dU_{xo}}{dy_2}, \quad \tilde{v}_2 = -\frac{\partial \tilde{A}}{\partial \tilde{z}} U_{zo}(y_2), \quad \tilde{w}_2 = \tilde{A}(\tilde{t}, \tilde{x}, \tilde{z}) \frac{dU_{zo}}{dy_2}, \tag{5.4a–c}$$

$$\tilde{\rho}_2 = \tilde{A}(\tilde{t}, \tilde{x}, \tilde{z}) \frac{dR_0}{dy_2}, \tag{5.4d}$$

$$\tilde{p}_2 = -\frac{\partial^2 \tilde{A}}{\partial \tilde{z}^2} \int_{y_2}^{\infty} R_0(Y_2) U_{zo}^2(Y_2) dY_2 \tag{5.4e}$$

where $-\tilde{A}$ denotes, as usual, the instantaneous displacement thickness. Actually, $\tilde{u}_2$ as given in (5.4*a*) separates from the other functions $\tilde{v}_2$, $\tilde{w}_2$, $\tilde{\rho}_2$ and $\tilde{p}_2$ which provide a two-dimensional model of crossflow disturbances at high Regnolds numbers.

Let us compare this model with one advanced by Messiter & Liñán (1976) in their study of laminar free convection developing in the proximity of a vertical flat plate and applied by Smith & Duck (1977) and Ryzhov (1982) to elucidating, respectively, separation and stability of a viscous near-wall jet. It is readily seen that the time, Cartesian coordinates and the corresponding velocities and excess pressure are scaled precisely in the same way in both asymptotic models under consideration. Then, (5.4*b*–*e*) yield the same two-dimensional solution for most of the boundary layer as that derived by Messiter & Liñán (1976), Smith & Duck (1977) and Ryzhov (1982) whereas an additional component $\tilde{u}_2$ of the velocity vector controls the disturbance pattern in the local streamwise direction depending on the basic spanwise motion. Thus, the crossflow acts like a spanwise near-wall jet in exciting unstable eigenmodes which may be isolated from streamwise oscillations. The distinctive feature to determine the crossflow jet-like behaviour stems from a mechanism underlying the self-induced pressure gradient: as (5.4*e*) shows it is supported by the local curvature $\partial^2 \tilde{A}/\partial \tilde{z}^2$ of streamsurfaces rather than by their slopes. The flow field in the upper deck remains unperturbed to leading order. That is why the pressure gradient is totally balanced by centrifugal forces in the main body of the boundary layer.

The characteristic thickness of the lower viscous sublayer is fixed by (5.1), therefore we may introduce here the scaled normal coordinate through $y' = \varepsilon^{36/7} \tilde{y}_3 = R^{-9/14} \tilde{y}_3$. The density does not vary within this sublayer, accordingly $\rho' = R_0(0) = (T_w^*/T_\infty^*)^{-1}$. The velocity field and pressure are represented in the form

$$(u', w') = \varepsilon^{8/7} (\tilde{u}_3, \tilde{w}_3) = R^{-1/7} (\tilde{u}_3, \tilde{w}_3), \tag{5.5a, b}$$

$$v' = \varepsilon^{20/7} \tilde{v}_3 = R^{-5/14} \tilde{v}_3, \quad p' = \varepsilon^{16/7} \tilde{p}_3 = R^{-2/7} \tilde{p}_3, \tag{5.5c, d}$$

again in keeping with Messiter & Liñán (1976), Smith & Duck (1977) and Ryzhov

(1982), and obey a system of asymptotic equations

$$\frac{\partial \tilde{v}_3}{\partial \tilde{y}_3} + \frac{\partial \tilde{w}_3}{\partial \tilde{z}} = 0, \tag{5.6a}$$

$$R_0(0)\left(\frac{\partial \tilde{u}_3}{\partial \tilde{t}} + \tilde{v}_3\frac{\partial \tilde{u}_3}{\partial \tilde{y}_3} + \tilde{w}_3\frac{\partial \tilde{u}_3}{\partial \tilde{z}}\right) = \frac{C}{R_0(0)}\frac{\partial^2 \tilde{u}_3}{\partial \tilde{y}_3^2}, \tag{5.6b}$$

$$R_0(0)\left(\frac{\partial \tilde{w}_3}{\partial \tilde{t}} + \tilde{v}_3\frac{\partial \tilde{w}_3}{\partial \tilde{y}_3} + \tilde{w}_3\frac{\partial \tilde{w}_3}{\partial \tilde{z}}\right) = -\frac{\partial \tilde{p}_3}{\partial \tilde{z}} + \frac{C}{R_0(0)}\frac{\partial^2 \tilde{w}_3}{\partial \tilde{y}_3^2} \tag{5.6c}$$

supplemented by $\partial\tilde{p}_3/\partial\tilde{y}_3 = 0$. Since (5.6*a, c*) do not contain $\tilde{u}_3$ these two equations separate from (5.6*b*) and can be integrated independently. Then $\tilde{u}_3$ is determined to set up the disturbance pattern in the local streamwise direction as dictated by the basic spanwise motion. An interaction law

$$\tilde{p}_3 = -D_{(zz)}\frac{\partial^2 \tilde{A}}{\partial \tilde{z}^2} \tag{5.7}$$

to connect the pressure with the displacement thickness as well as limiting conditions

$$\tilde{u}_3 - \tilde{y}_3 \mathrm{d}U_{xo}(0)/\mathrm{d}y_2 \longrightarrow \tilde{A}(\tilde{t},\tilde{x},\tilde{z})\mathrm{d}U_{xo}(0)/\mathrm{d}y_2, \tag{5.8a}$$

$$\tilde{w}_3 - \tilde{y}_3 \mathrm{d}U_{zo}(0)/\mathrm{d}y_2 \longrightarrow \tilde{A}(\tilde{t},\tilde{x},\tilde{z})\mathrm{d}U_{zo}(0)/\mathrm{d}y_2 \tag{5.8b}$$

at the upper reaches $\tilde{y}_3 \to \infty$ of the lower viscous sublayer come from matching (5.5*a–d*) to (5.3*a–d*), $D_{(zz)}$ being defined in (3.14*c*). In addition, the conventional no-slip conditions

$$\tilde{u}_3 = \tilde{v}_3 = \tilde{w}_3 = 0 \tag{5.9}$$

hold at the solid surface $\tilde{y}_3 = 0$.

An affine transformation allows us to exclude all the parameters C, $R_0(0)$, $D_{(zz)}$, $\mathrm{d}U_{xo}(0)/\mathrm{d}y_2$ and $\mathrm{d}U_{zo}(0)/\mathrm{d}y_2$ from the governing equations (5.6*a–c*), interaction law (5.7) and constraints (5.8*a, b*) to be met as $\tilde{y}_3 \to \infty$. However, since our aim is deriving a set of composite equations and boundary conditions which might be employed to cover both moderate values of the frequency and wavenumbers and the extreme case involving indefinitely large frequencies and wavenumbers we omit details and restrict ourselves to fundamental properties inherent in the jet-like crossflow.

According to Smith & Duck (1977), the boundary-value problem formulated controls separation from a side part of a vortex elongated in the streamwise direction. On the other hand, Ryzhov (1982) pointed out that the model (5.6*a, c*), (5.7), (5.8*b*) and (5.9) leads to unstable eigenmodes. However, in the framework of this model the disturbance amplitude growth rate proves to decay as the wavenumber tends to infinity. Hence the Cauchy problem remains well posed in the limiting case under consideration. The new effects entering at high wavenumbers were also treated in a relevant study by Davis (1992). However, the asymptotic system of equations appears in that work in a form somewhat different from (5.6*a–c*) and (5.7).

6. Composite asymptotic model

As has been mentioned in the preceding section, a singularity in the real part of ω_1 ensuing from (4.10*a, b*) implies that a typical value of the frequency in this limiting case becomes $\omega_1 \sim O(\varepsilon^{-1})$ while both wavenumbers $k = k_0$ and $m = m_0$ are kept fixed. It is possible to show that this singularity causes a critical layer to form at some distance from a solid surface. Insofar as the Cauchy problem remains well posed we leave aside an in-depth analysis of the corresponding disturbance pattern.

Let us incorporate the second, and even stronger, singularity occurring in the imaginary part of ω_1 into the composite asymptotic model. The way to remove this singularity in the limit as both wavenumbers k and m tend to infinity has been thoroughly analysed in the preceding Section. When devising an extended theory we may proceed in an analogous manner. However, there is a point of nicety to be elucidated at first. By virtue of (5.2b, d) characteristic values of x_m and z_m in the limiting case become $O(R^{-11/28})$ and $O(R^{-12/28})$, respectively. On the assumption that $R \to \infty$ they prove to be much larger than a reference wavelength of order $R^{-9/20}$ intrinsic to disturbances from the vicinity of the upper branch of the neutral stability curve (Bodonyi & Smith 1981; Zhuk & Ryzhov 1983). So, our consideration is not beyond the scope of the triple-deck approach. Next, on the strength of (5.1) a typical thickness of the near-wall viscous sublayer can be estimated as $O(R^{-9/14})$. Asymptotically this region is located beneath the critical layer of the upper-branch disturbances that lies at a distance $O(R^{-11/20})$ from the solid surface. What is more, in the limiting case in question the near-wall viscous sublayer turns out to be submerged in the lower deck of the conventional triple-deck structure. In consequence the flow pattern as a whole remains intact even if an extended version of the triple-deck theory has to encompass (and mitigate) the stronger singularity. However, in practical terms the distinctions between all of the aforementioned characteristic lengths are small and hardly discernible at values of the Reynolds number in the range of transition.

It follows from the foregoing that the self-induced pressure in the form of (2.6) controls the potential flow region. The velocity and density fields in the main deck obey the expressions

$$u_2 = A_m(t_m, x_m, z_m)\frac{\mathrm{d}U_{xo}}{\mathrm{d}y_2}, \quad w_2 = A_m(t_m, x_m, z_m)\frac{\mathrm{d}U_{zo}}{\mathrm{d}y_2}, \tag{6.1a,b}$$

$$v_2 = -\frac{\partial A_m}{\partial x_m}U_{xo}(y_2) - \frac{\partial A_m}{\partial z_m}U_{zo}(y_2), \tag{6.1c}$$

$$\rho_2 = A_m(t_m, x_m, z_m)\frac{\mathrm{d}R_0}{\mathrm{d}y_2} \tag{6.1d}$$

analogous to (5.4a–d). A distinction arises from the dependence of v_2 on both velocity profiles U_{xo} and U_{zo} rather than owing to accounting for the second-order terms in (2.9). However, the leading of the second-order terms in (2.8) determines a non-vanishing normal component of the pressure gradient

$$\varepsilon U_{zo}\frac{\partial v_2}{\partial z_m} = -\frac{1}{R_0}\frac{\partial p_2}{\partial y_2} \tag{6.2}$$

in keeping with the analysis set forth in §5. Integrating (6.2) results in

$$p_2 = p_{2\infty}(t_m, x_m, z_m) - \varepsilon\frac{\partial^2 A_m}{\partial z_m^2}\int_{y_2}^{\infty} R_0(Y_2)U_{zo}^2(Y_2)\mathrm{d}Y_2 \tag{6.3}$$

with an additional term $p_{2\infty}(t_m, x_m, z_m)$ on the right-hand side as compared to the limiting case (5.4e). No other terms in the main deck stem from allowing for the second singularity. The near-wall viscous sublayer is governed by (2.12a–c) as before.

Let us introduce the normalized displacement thickness $-A$ by means of

$$A_m = \tau_w^{-3/4}C^{5/8}(T_w^*/T_\infty^*)^{3/2}A \tag{6.4}$$

and go over from a frame of reference (t_m, x_m, z_m) to a system of canonical variables t, x, z. Then the matching of (6.1*c*), as $y_2 \to \infty$, to the normal velocity at the bottom of the outer deck provides a condition

$$\frac{\partial \varphi_1}{\partial y_1} = -\frac{\partial A}{\partial x} \quad \text{at} \quad y_1 = 0, \tag{6.5}$$

with y_1 defined in (2.2), to be introduced into (2.6). The form of (6.5) is precisely the same as the one adopted in the classical triple-deck theory. Using (6.5) we infer from the matching of the pressures in two regions under consideration that

$$p_{2\infty}(t,x,z) = -\tau^{1/2}C^{1/4}\frac{1}{2\pi}\int_{-\infty}^{\infty}\mathrm{d}\xi\int_{-\infty}^{\infty}\frac{\partial^2 A(t,\xi,\zeta)/\partial\xi^2}{\left[(x-\xi)^2+\left(1-M_\infty^2\right)(z-\zeta)^2\right]^{1/2}}\mathrm{d}\zeta \tag{6.6}$$

All that remains to be done is to match solutions for the main deck and the near-wall viscous sublayer. Following the standard procedure, as applied to (6.1*a, b*), and using definitions (1.1*a, b*) of τ_x and τ_z we arrive at conditions

$$u_3 - \tau_x y_3 \to \tau_x A, \quad w_3 - \tau_z y_3 \to \tau_z A \qquad \text{as} \quad y_3 \to \infty \tag{6.7a, b}$$

for velocity components in a horizontal plane. Next, since $p_3 = \tau_w^{-1/2}C^{-1/4}p_2$, as $y_2 \to 0$, an expression for the pressure across the near-wall sublayer can be obtained relying on (6.3) with A_m transformed to A through (6.4). From (6.6) we find that

$$p_3 = -\frac{1}{2\pi}\int_{-\infty}^{\infty}\mathrm{d}\xi\int_{-\infty}^{\infty}\frac{\partial^2 A(t,\xi,\zeta)/\partial\xi^2}{\left[(x-\xi)^2+\left(1-M_\infty^2\right)(z-\zeta)^2\right]^{1/2}}\mathrm{d}\zeta - \varepsilon_2 D_{(zz)}\frac{\partial^2 A}{\partial z^2} \tag{6.8}$$

where the small parameter $\varepsilon_2 = \varepsilon\tau_w^{5/4}C^{-3/8}(T_w^*/T_\infty^*)^{-3/2}$. Notice that the limiting conditions (6.7*a, b*) at the upper reaches of the near-wall sublayer acquire precisely the same form as they take within the framework of the conventional triple-deck theory. To the contrary, the generalized interaction law (6.8) involves an additional term that stems from accounting for centrifugal forces due to the local curvature of streamsurfaces in most of the boundary layer. As usual, variations of p_3 are to be found simultaneously with the velocity field u_3, v_3, w_3 and the instantaneous displacement thickness A by integrating the system (2.12*a–c*) subject to the limiting conditions (6.7*a, b*), as $y_3 \to \infty$, and the no-slip conditions $u_3 = v_3 = w_3 = 0$ at the flat plate $y_3 = 0$. Thus, the composite asymptotic model sought is complete. Disturbances of a different nature, including travelling waves and crossflow vortices are coupled together within the new model.

In searching for a linear solution of the travelling-wave type we use (3.1) and decompose A in a similar way:

$$A = A_0 \exp[\mathrm{i}(\omega t + kx + mz)]. \tag{6.9}$$

However, a brief inspection of the solution in the main deck proves to be instrumental in elucidating an important feature of the model. Making use of the matching condition (6.5), as applied to (3.6*a, b*), (3.7) and (6.1*c*), (6.9), results in an expression

$$g_2 = -\mathrm{i}\tau_w^{1/2}C^{1/4}p_{10}\left(kU_{xo} + mU_{zo}\right)\frac{\ell}{k^2} \tag{6.10}$$

that is nothing other than the leading-order term of the general relationship (3.11*a*).

Next, (6.1a,b) reduce to

$$f_2 = \mathrm{i}\tau_w^{-5/4} C^{3/8} \left(\frac{T_w^*}{T_\infty^*}\right)^{3/2} \frac{\mathrm{d}U_{xo}}{\mathrm{d}y_2} \frac{g_2}{kU_{xo} + mU_{zo}}, \tag{6.11a}$$

$$h_2 = \mathrm{i}\tau_w^{-5/4} C^{3/8} \left(\frac{T_w^*}{T_\infty^*}\right)^{3/2} \frac{\mathrm{d}U_{zo}}{\mathrm{d}y_2} \frac{g_2}{kU_{xo} + mU_{zo}}, \tag{6.11b}$$

giving the leading-order terms of (3.15a,b), respectively. Thus, the formation of a critical layer is not allowed in the context of the composite model since the ratio $g_2/(kU_{xo}+mU_{zo})$ remains finite for any y_2 on the strength of (6.10). The corresponding assumption has been made in §2 in order to substantiate the replacement of p_2 in (2.9) by its limiting value $p_{2\infty}$ at the outer edge of the main deck.

In the limit as $y_3 \to \infty$ we get both $f \to A_0$ and $h \to A_0$ by virtue of (6.7a,b), hence $F \to KA_0$ in agreement with the conventional triple-deck approach. A relation

$$p_{30} = A_0 \left(\frac{k^2}{\ell} + \varepsilon_2 m^2 D_{(zz)}\right) \tag{6.12}$$

between the constants p_{30} and A_0 comes from the interaction law (6.8). The second term in the brackets on the right-hand side of (6.12) gives a contribution from centrifugal forces supported by the local curvature $\partial^2 A/\partial z^2$ of streamsurfaces. Eliminating A_0 between $F(\infty) = KA_0$ and (6.12) we derive from (3.17a) a dispersion relation

$$\Phi(\Omega) = \frac{\mathrm{i}^{1/3}(k^2+m^2)}{K^{5/3}} \left(\frac{k^2}{\ell} + \varepsilon_2 m^2 D_{(zz)}\right) \tag{6.13}$$

with Φ defined by (3.17b). It is necessary now to put linear properties of the composite model, governed by the modified dispersion relation, to a test.

The singularity in $\mathrm{Re}(\omega_1)$ responsible for the high-frequency behaviour in the limit as $K \to 0$ and $k \to k_0, m \to m_0$ remains not affected to leading order. The term proportional to ε_2 on the right-hand side of (6.13) contributes only a small correction to the first root ω_1, thus (4.10a,b) still hold. As mentioned above, the singularity in $\mathrm{Re}(\omega_1)$ causes a critical layer to be formed in the disturbance field. The flow pattern that results is beyond the scope of present analysis.

When analysing the second, and much stronger, singularity leading to ill-posedmess of the Cauchy problem within the framework of the conventional triple-deck theory we need to keep in mind that preserving a correction term in the interaction law (6.8) and ensuing dispersion relation (6.13) entails the first-order contribution to ω_1 when both wavenumbers k and m tend to infinity. Even with the correction term present, (6.13) can be studied using the same symmetry properties that are intrinsic to (4.4) and specified in (4.5) and (4.6). This makes it possible to take full advantage of results for the complex Ω-plane set forth in §4 and apply them to tackling the most important issue on contours of $\mathrm{Im}(\omega_1)$ under the assumption that k and m are real. In the limiting case $\varepsilon_2 = 0$ these lines are plotted in figure 3 for $M_\infty = 0.2$, $\tau_x = \sqrt{8}/3$, $\tau_z = 1/3$, and of particular interest is an image of the neutral stability curve $\mathrm{Im}(\omega_1) = 0$ whose asymptotes $m = \pm 0.999\tau_z^{-5/2}k^3$ stretch to infinity in the (k,m)-plane, as $k \to \infty$. However, the shape of the contours far from the origin dramatically changes if $\varepsilon_2 \neq 0$. This may be concluded from figure 4 drawn for the same values of M_∞, τ_x, τ_z but with $\varepsilon_2 = 0.001$. Here the symmetry properties (4.5) and (4.6) are easily recognizable again. Two local negative minima of $\mathrm{Im}(\omega_1)$ and a local negative maximum in between are even more clear cut in figure 4 as compared with

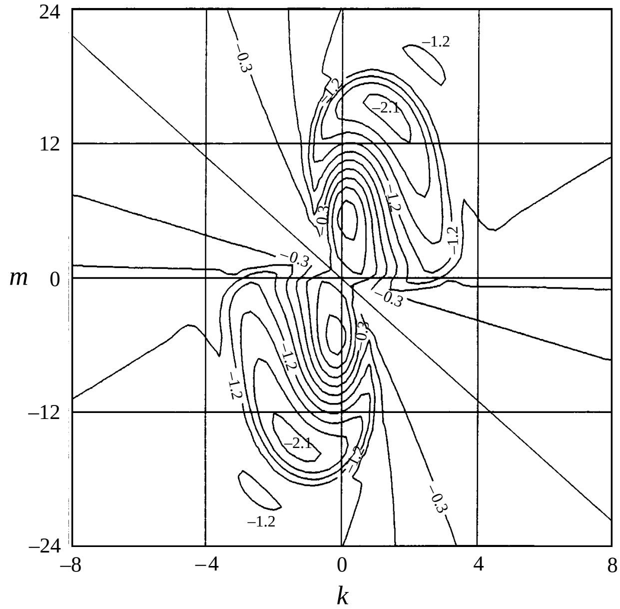

FIGURE 4. Contours of Im(ω_1) in the real (k, m)-plane formed by both wavenumbers under the extended asympototic model; $\varepsilon_2 = 0.001, M_\infty = 0.2, \tau_x = \sqrt{8}/3, \tau_z = 1/3$.

analogous extrema of the same function shown in figure 3. In consequence of a new structure of the (k, m)-plane, the asymptotic behaviour of the disturbance amplitude growth rate becomes different from one intrinsic to the limiting case $\varepsilon_2 = 0$. To prove this statement let $m = ck^3$, $k \to \infty$ in (6.13). As a result the dispersion-relation root ω_1 is given by

$$\omega_1 = -\varepsilon_2 c^3 \tau_z^{-1} D_{(zz)} k^9 - \frac{\sqrt{2}}{2}(1+\mathrm{i})\varepsilon_2^{-1/2} c^{-1/2} \tau_z^{3/2} D_{(zz)}^{-1/2} k^{-3/2} \tag{6.14}$$

in the first two approximations provided that $\varepsilon_2 c^3 k^7 \gg 1$. It should be pointed out that (6.14) ensues from the analysis presented in §5 for $k \sim \varepsilon^{-1/7}$ (see also Ryzhov 1982). Thus, the amplitude growth rate of self-excited modes turns out to be bounded for any k and tends to zero as $k \to \infty$. The Cauchy problem becomes well posed within the framework of the composite asymptotic model developed where allowance for centrifugal forces is a crucial element in suppressing unrealistic amplification of short-scaled disturbances.

Images of the neutral stability curve Im(ω_1) = 0 in the upper half-plane of the real (k, m)-plane are depicted in figure 5 for different values of ε_2. A curve that corresponds to the limiting case $\varepsilon_2 = 0$ is labelled 0, and in compliance with the foregoing their asymptotes stretch to infinity indefinitely, approaching $m = \pm 0.999\tau_z^{-5/2}k^3$ as $k \to \infty$. However, with $\varepsilon_2 \neq 0$ all the other curves numbered 1, 2, 3 are closed loops. The greater the value taken by ε_2, the smaller are dimensions of the loops (in fact the spanwise wavenumber m does not exceed 5 even if ε_2 remains as small as 0.01). Thus, the effects of centrifugal forces are twofold: they make a domain of stable eigen-oscillations bounded in the (k, m)-plane, and the amplitude growth rate of self-excited modes remains finite with $k \to \infty$. Further inspection of (6.14) discloses that stable oscillations are realized solely when $c \to \infty$.

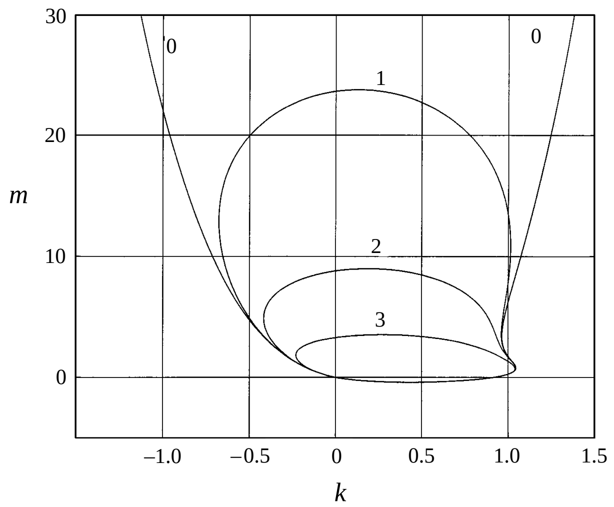

FIGURE 5. The shapes of the neutral stability curve $\mathrm{Im}(\omega_1) = 0$ in the real (k, m)-plane for $M_\infty = 0.2, \tau_x = \sqrt{8}/3, \tau_z = 1/3$; curve $0, \varepsilon_2 = 0; 1, \varepsilon_2 = 10^{-4}; 2, \varepsilon_2 = 10^{-3}; 3, \varepsilon_2 = 10^{-2}$.

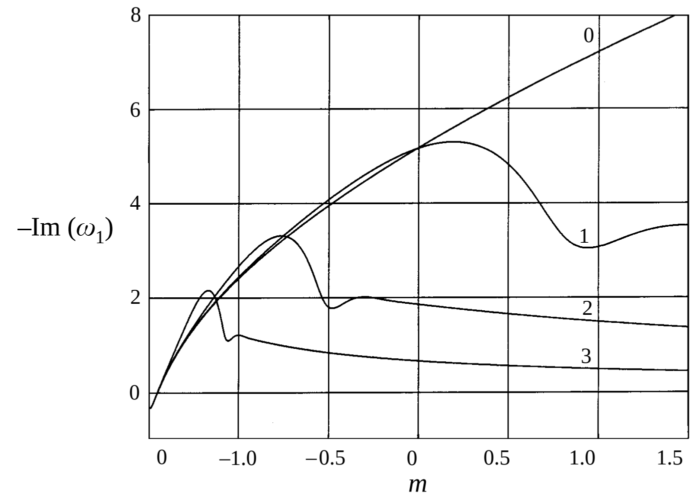

FIGURE 6. The amplitude growth rate, $-\mathrm{Im}(\omega_1)$, as a function of the spanwise wavenumber for $M_\infty = 0.2, \tau_x = \sqrt{8}/3, \tau_z = 1/3$; curve $0, \varepsilon_2 = 0; 1, \varepsilon_2 = 10^{-4}; 2, \varepsilon_2 = 10^{-3}; 3, \varepsilon_2 = 10^{-2}$. All the curves shown are calculated on the assumption that the trajectory $m = 0.1356\tau_z^{-5/2}k^3$ corresponds to the maximum amplification in the limiting case $\epsilon_2 = 0$.

The disturbance amplitude growth rate fixed by $-\mathrm{Im}(\omega_1)$ is shown in figure 6 for different values of ε_2 as a function of the spanwise wavenumber m. All the curves here are obtained on the assumption that the trajectory $m = c_2^* k^3 = 0.1356\tau_z^{-5/2}k^3$ corresponding to the maximum amplification in the limiting case $\varepsilon_2 = 0$ is chosen in the (k, m)-plane. The curve labelled 0 relates to $\varepsilon_2 = 0$, so it may be regarded as an outcome of the conventional triple-deck theory. Accordingly, the amplitude growth rate tends to infinity as $m \to \infty$. The other curves marked 1, 2, 3 are calculated with $\varepsilon_2 \neq 0$. Their behaviour suggests that self-excited disturbances are amplified within certain bounds for all m, and

$$\mathrm{Im}(\omega_1) = -\frac{\sqrt{2}}{2}\varepsilon_2^{-1/2}\tau_z^{3/2}D_{zz}^{-1/2}m^{-1/2} \qquad \text{as} \quad m \to \infty, \tag{6.15}$$

in view of (6.14). The passage to the limit $\varepsilon_2 \to 0$ is non-uniform: the smaller is a value of the parameter, the greater are spanwise wavenumbers required for achieving the final attenuation of $\mathrm{Im}(\omega_1)$. However, the asymptotic decay $\mathrm{Im}(\omega_1) \to 0$, as $m \to \infty$, ensues from (6.15) no matter how small (but fixed) ε_2 may be.

7. Concluding remarks

Results presented above for a steady subsonic three-dimensional boundary-layer flow on a flat plate allow us to isolate TS and crossflow instabilities from leading-edge contamination and Görtler vortices developing on the blunt nose of a swept wing. The former two instabilities turn out generally to be interconnected and inseparable, i.e. TS waves and crossflow vortical disturbances interact and grow simultaneously. However, crossflow instability becomes dominant if both wavenumbers tend to infinity, being tied by a certain relation. In this limiting case a set of simplified equations controls the wave pattern developing in the spanwise direction. Here the dominant fluid motion occurs in the form of a jet-like near-wall flow. This flow is driven by the self-induced pressure gradient (5.7) balancing centrifugal forces arising owing to the large curvature of streamsurfaces in the main deck. TS waves propagating in the streamwise direction exert no influence on the spanwise jet-like disturbances and do not contribute, to leading order, to their amplification. On the other hand, the excitation and growth of crossflow oscillations strongly affect the mechanism of TS instability. The dominant short-scale spanwise motion in a three-dimensional boundary layer bears a close resemblance to a viscous jet spreading along a solid flat plate (Smith & Duck 1977; Ryzhov 1982).

As is known from Zhuk & Ryzhov (1982), Smith & Burggraf (1985) and Kachanov, Ryzhov & Smith (1993), the triple-deck regime of viscous/inviscid interaction gives way to an essentially nonlinear soliton stage when the wave amplitude attains values measured in terms of a parameter $\varDelta$ such that $\varepsilon \ll \varDelta \ll 1$. A new adjustment sublayer is embedded between the main deck and near-wall sublayer at this stage of short-scaled crossflow oscillations. The disturbance pattern within the adjustment sublayer proves to be inviscid and is obtainable by solving a system of boundary-layer-type equations (5.6a,c) with $\partial^2\tilde{w}_3/\partial\tilde{y}_3^2$ omitted on the right-hand side of the latter. In appropriately scaled and normalized variables a desired solution to the simplified equations reads (Zhuk & Ryzhov 1982; Smith & Burggraf 1985)

$$\tilde{w}_3 = \tilde{y}_3 + \tilde{A}, \quad \tilde{v}_3 = -\tilde{y}_3\frac{\partial \tilde{A}}{\partial \tilde{z}} - \frac{\partial \tilde{A}}{\partial \tilde{t}} - \tilde{A}\frac{\partial \tilde{A}}{\partial \tilde{z}} - \frac{\partial \tilde{p}_3}{\partial \tilde{z}} \tag{7.1a,b}$$

where $\tilde{A}_w = \tilde{A} + y_w$ comes from

$$\frac{\partial \tilde{A}_w}{\partial \tilde{t}} + \tilde{A}_w\frac{\partial \tilde{A}_w}{\partial \tilde{z}} = \frac{\partial^3 \tilde{A}_w}{\partial \tilde{z}^3} - f, \quad f = \frac{\partial^3 \tilde{y}_w}{\partial \tilde{z}^3} \tag{7.2a,b}$$

in view of the interaction law (5.7), $\tilde{y}_w = \tilde{y}_w(\tilde{t},\tilde{z})$ being the shape of a local uneveness on an otherwise flat plate. Thus, the generation of coherent nonlinear crossflow structures can be studied using (7.1a,b) with the instanteneous displacement thickness $-\tilde{A}$ determined by both periodic and solitary-like wave solutions of the famous Korteweg–de Vries equation. It is an intricate unsteady motion that generally emerges even if a forcing f in the inhomogeneous model (7.2a, b) is assumed to be independent of time.

The authors would like to express their sincere gratitude to Professor Julian D. Cole for many discussions and encouraging comments. Special thanks are also due to Drs Marvin E. Goldstein and Stephen J. Cowley for their positive criticisms. The study has been carried out with the support to O.S.R. of AFOSR under grant F49620-93-1-0022DEF and to E.D.T. of NAS under CAST grants.

REFERENCES

Arnal, D. 1986 Three-dimensional boundary layers: Laminar-turbulent transition. *AGARD Rep.* 741 (Special course on calculation of three-dimensional boundary layers with separation). Von Kármán Inst., Rhode-St.-Genese, Belgium.

Arnal, D. & Juillen, J. C. 1987 Three-dimensional transition studies at ONERA/CERT. *AIAA Paper* 87-1335.

Bodonyi, R. J. & Smith, F. T. 1981 The upper branch stability of the Blasius boundary layer, including non-parallel flow effects. *Proc. R. Soc. Lond.* A **375**, 65–92.

Cebeci, T. & Stewartson, K. 1980 On stability and transition in three-dimensional flows. *AIAA. J.* **18**, 398–405.

Choudhari, M., Hall, P. & Streett, C. 1994 On spatial evolution of long-wavelength Görtler vortices governed by a viscous-inviscid interaction. Part I: The linear case. *Q. J. Mech. Appl. Maths* **47**, 207–229.

Davis, D. A. R. 1992 On linear and nonlinear instability in boundary layers with crossflow. PhD Thesis, University College London.

Gray, W. E. 1952 The effect of wing sweep on laminar flow. *RAE TM Aero.* 255.

Grecory, N., Stuart, J. T. & Walker, W. S. 1955 On the stability of three-dimensional boundary layers with applications to the flow due to a rotating disk. *Phil. Trans. R. Soc. Lond.* A **248**, 155–199.

Hefner, J. N. & Bushnell, D. M. 1980 Status of linear boundary-layer stability theory and the e^N method, with emphasis on swept-wing applications. *NASA TP*-1645.

Kachanov, Yu. S., Ryzhov, O. S. & Smith, F. T. 1993 Formation of solitons in transitional boundary layers: theory and experiment. *J. Fluid Mech.* **191**, 273–297.

Kachanov, Yu. S., Tararykin, O. I. & Fedorov, A. V. 1990 A study of the stability of a boundary layer on a swept-wing model against stationary disturbances. *Izv. Sibirsk. Otd. Akad. Nauk SSSR. Tekh. Nauk.* No. 5, 11–21 (in Russian).

Lingwood, R. J. 1995 Absolute instability of the boundary layer on a rotating disk. *J. Fluid Mech.* **299**, 17–33.

Mack, L. M. 1984 Boundary-layer linear stability theory. *AGARD Rep.* 709 (Special course on stability and transition of laminar flows). Von Kármán Inst., Rhode-St.-Genese, Belgium.

Manuilovich, S. V. 1983 On the free interaction of a spatial boundary layer with an external potential flow. *Izv. Akad. Nauk SSSR, Mekhan. Zhidk. i Gaza* No. 5, 45–53 (in Russian; English transl. *Fluid Dyn.* **18**, 695–701, 1984).

Messiter, A. F. 1970 Boundary-layer flow near the trailing edge of a flat plate. *SIAM J. Appl. Math.* **18**, 241–257.

Messiter, A. F. & Liñán, A. 1976 The vertical plate in laminar free convection: effects of leading and trailing edges and discontinuous temperature. *Z. Angew. Math. Phys.* **27**, 633–651.

Nitschke-Kowsky, P. & Bippes, H. 1988 Instability and transition of a three-dimensional boundary layer on a swept flat plate. *Phys. Fluids* **31**, 786–795.

Poll, D. I. A. 1985 Some observations of the transition process on the windward face of a long yawed cylinder. *J. Fluid Mech.* **150**, 329–356.

Reed, H. L. & Saric, W. S. 1989 Stability of three-dimensional boundary layers. *Ann. Rev. Fluid Mech.* **21**, 235–284.

Ruban, A. I. 1990 Propagation of wave packets in the boundary layer on a curved surface. *Izv. Akad. Nauk SSSR, Mekhan. Zhidk. i Gaza* No. 2, 59–68 (in Russian; English transl. *Fluid Dyn.* **25**, 213–221, 1990).

Ryzhov, O. S. 1982 Instability of a viscous near-wall jet. *Zh. Prikl. Mekh. Tekh. Fiz.* No. 2, 26–33 (in Russian; English transl. *J. Appl. Mech. Tech. Phys.* **23**, 181–187, 1982).

Ryzhov, O. S. 1993 An asymptotic approach to stability problems of a transonic boundary layer. In *Transonic Aerodynamics. Problems in Asymptotic Theory* (ed. L. P. Cook), pp. 29–53. SIAM.

Ryzhov, O. S. & Terent'ev, E. D. 1986 On the transition mode characterizing the triggering of a vibrator in the subsonic boundary layer on a plate. *Prikl. Matem. Mekham.* **50**, 974–986 (in Russian; English transl. *PMM USSR* **50**, 753–762, 1986).

Ryzhov, O. S. & Terent'ev, E. D. 1991 Wave motions in a three-dimensional boundary layer. *Prikl. Matem. Mekhan.* **55**, 912–927 (in Russian; English transl. *PMM USSR* **55**, 789–804, 1991).

Saric, W. S. & Yeates, L. G. 1985 Experiments on the stability of crossflow vortices in swept-wing flows. *AIAA Paper* 85-0493.

Savenkov, I. V. 1990 Instability of a boundary layer on a curved surface. *Izv. Akad. Nauk SSSR, Mekhan. Zhidk. i Gaza* No. 1, 176–179 (in Russian; English transl. *Fluid Dyn.* **25**, 151–154, 1990).

Smith, A. M. O. & Gamberoni, N. 1956 Transition, pressure gradient, and stability theory. *Douglas Aircraft Co., Inc., ES* 26388.

Smith, F. T. 1989 On the first-mode instability in subsonic, supersonic or hypersonic boundary layers. *J. Fluid Mech.* **198**, 127–153.

Smith, F. T. & Burggraf, O. R. 1985 On the development of large-sized short-scaled disturbances in boundary layer. *Proc. R. Soc. Lond.* A **399**, 25–55.

Smith, F. T. & Duck, P. W. 1977 Separation of jets or thermal boundary layers from a wall. *Q. J. Mech. Appl. Math.* **30**, 143–156.

Smith, F. T., Sykes, R. I. & Brighton, P. W. 1977 A two-dimensional boundary layer encountering a three-dimensional hump. *J. Fluid Mech.* **83**, 163–176.

Squire, H. B. 1933 On the stability of three-dimensional disturbances of viscous fluid flow between parallel walls. *Proc. R. Soc. Lond.* A **142**, 621–628.

Stewart, P. A. & Smith, F. T. 1987 Three-dimensional instabilities in steady and unsteady non-parallel boundary layers, including effects of Tollmien-Schlichting disturbances and crossflow. *Proc. R. Soc. Lond.* A **409**, 229–248.

Stewartson, K. 1969 On the flow near the trailing edge of a flat plate. II. *Mathematika* **16**, 106–121.

Van Ingen, J. L. 1956 A suggested semi-empirical method for the calculation of the boundary-layer transition region. *Reps. VTH 71, 74,* Dept. Aeronaut. Eng., Univ. Technol., Delft, Netherlands.

Zhuk, V. I. & Ryzhov, O. S. 1982 Locally inviscid perturbations in a boundary layer with self-induced pressure. *Dokl. Akad. Nauk SSSR*, **263**, 56–59 (in Russian; English transl. *Sov. Phys. Dokl.* **27**, 177–179, 1982).

Zhuk, V. I. & Ryzhov, O. S. 1983 Asymptotic behaviour of solutions to the Orr-Sommerfeld equation which control unsteady oscillations at high values of the Reynolds number. *Dokl. Akad. Nauk SSSR*, **268**, 1328–1332 (in Russian; English transl. *Sov. Phys. Dokl.* **28**, 87–89, 1983).